Sol-Gel Transition in Agar-Gelatin Mixtures Studied with Transient Elastography

Jean-Luc Gennisson and Guy Cloutier, *Member, IEEE*

Abstract—Using the shear wave propagation in solids, the transient elastography technique has been developed to assess the elastic properties of soft tissues. Here, a new approach of transient elastography allows assessing the viscoelastic properties of soft tissues. In this paper, the method is used to follow-up the sol-gel transition of an agar-gelatin mixture noninvasively. The shear wave velocity and shear wave attenuation through the mixture were continuously monitored in the audible range of frequencies (from 50 Hz to 200 Hz). The observed changes in velocities and attenuations as a function of frequency confirmed the validity of the Voigt's model to describe the gel at its stable mechanical state. By a simple inverse problem approach, based on the one-dimensional (1-D) Helmholtz equation, the elasticity and the viscosity of such a mixture were recovered as a function of time. The results obtained are in good agreement with the literature and theoretical predictions. Overall, they demonstrate the high sensitivity of the transient elastography measurements to the rheological parameter changes in agar-gelatin mixtures during gelation.

I. Introduction

THE sol-gel processes have attracted attention for several decades. To describe this transition from liquid (sol) to solid (gel), some basic theories were developed [1]–[4]. Winter and Chambon [5], [6] proposed a new theory to describe the time evolution of the complex shear modulus G in polymer mixtures. From a phenomenological point of view, the sol-gel transition is characterized by an increase of the elasticity and viscosity as a function of time. Many ways have been developed to assess the mechanical properties of polymer during sol-gel transition. For a wide array of frequency ranges, several methods can be used. At low frequencies (from 10^{-6} Hz to 1 Hz), rheological measurements and flow relaxation techniques were proposed [7]–[9]. Thermodynamic analysis techniques and resonance frequencies are used in the range from 10^{-2} Hz to 1 kHz [10]. In the specific audible range, from 10 Hz to 30 kHz, only two techniques were developed, photoacoustic spectroscopy using a YAG (yttrium aluminum garnet) laser [11] or the acoustic method [12]. In the first, the YAG laser light is absorbed by a black carbon layer used as a

beaker. The acoustic waves generated by heat emission are detected by a microphone placed at the sample surface. In the second, a transducer (bandwidth from 0.3 to 30 kHz) is applied at the surface of the medium to generate acoustic waves through the sol-gel mixture that are detected by a microphone placed in front of it. Between 100 kHz and 100 MHz, ultrasonic methods are used [13]. The ultrasonic wave amplitude and velocity measurements allow one to assess the material mechanical properties. Over this range of frequencies (above 100 MHz), optical methods were developed [14].

In the field of dynamic elastography, which occurs in the audible frequency range, only magnetic resonance imaging was recently used to assess the sol-gel transition [15]. In the current paper, a new ultrasound-based technique called transient elastography is presented to retrieve the mechanical properties of sol-gel transition of agar-gelatin mixtures. By using the one-dimensional (1-D) shear elasticity probe, the propagation of shear waves in the audible range of frequencies is followed instantaneously [16]. This technique showed its efficiency to retrieve the anisotropic [17], nonlinear [18]–[20] or viscoelastic [21] properties of biological soft tissues.

In term of viscoelastic properties, it has been shown that the shear elasticity probe allows one to map the viscosity of soft tissues. Experimental results on beef muscles *in vitro* and agar-gelatin phantoms pointed out that the Voigt's model is appropriate to describe the soft solid viscoelasticity [21]. The use of a simple inverse problem approach based on the 1-D Helmholtz equation confirmed this choice. Thus, it is possible to retrieve the elasticity (μ) and viscosity (η) of the investigated media.

Here, this method is used to follow the sol-gel transition of agar-gelatin mixtures. The shear wave velocity and attenuation are studied as a function of the gelatin concentration, shear wave amplitude, and frequency.

II. Materials and Methods

A. Materials

The shear elasticity probe was used in the present experimental study [16]. It is composed of a single element, 10 MHz, ultrasonic transducer (Panametrics, model V312, Waltham, MA) mounted on a minishaker (Brüel & Kjær, type 4810, Nærum, Denmark). The shear waves were generated by the front face of the transducer; meanwhile, it was working in a pulse-echo mode. The ultrasound longitu-
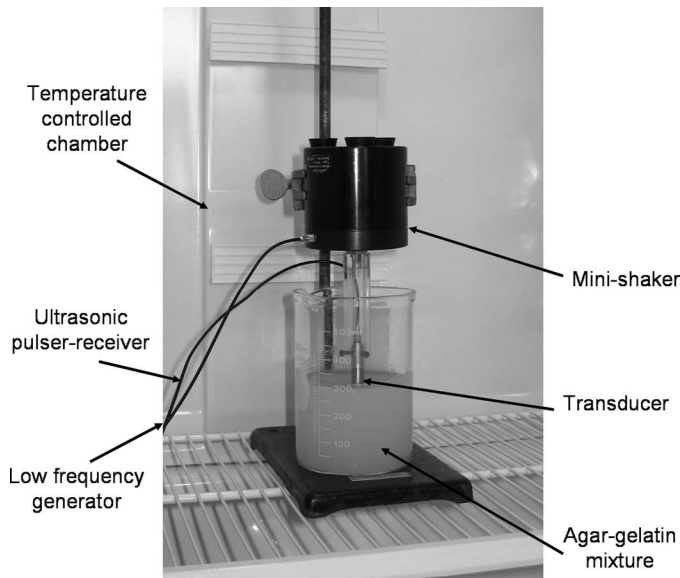
Fig. 1. Experimental setup, the shear elasticity probe was composed of a transducer mounted on a minishaker. The probe was placed in a temperature-controlled chamber at the surface of an agar-gelatin mixture in a liquid state. The gel solidification was followed for 12 hours.

dinal waves were generated by a pulsed-echo system (Panametrics, model 5900PR, Waltham, MA) and the low frequency pulse (from 50 to 200 Hz), producing shear waves, were sent to the minishaker with a function generator (Agilent, model 33250A, Palo Alto, CA) and amplified (Brüel & Kjær, type 2706, Nærum, Denmark). In a typical experiment, 300 echographic lines were recorded in an eight bit format with an acquisition card (Gage, type Compuscope 8500, Lachine, QC, Canada) on a personal computer at a 100 MHz sampling frequency. The repetition frequency between successive A-scans was fixed in the experiments at 2 kHz.

Agar-gelatin samples were a mixture of water (initially heated at $50°C$), 3% agar (Sigma Chemical, number A-6924, Saint-Louis, MO), and 1.5% to 4% gelatin (Sigma Chemical, number G-2500 Type A from porcine skin, Saint-Louis, MO). The agar and gelatin were used as scatterers and matrix, respectively. At this temperature, the agar was not dissolved (the agar melting point is about $85°C$). The phantom speckle is provided by the agar particles so, if they are dissolved, one cannot get ultrasonic signals.

The usual control temperature for this kind of experiment has been made as follows [22]: at the beginning, the agar-gelatin mixture was in a liquid state, and its temperature was reduced from $50°C$ to $24°C$. Then to control the sol-gel transition and to avoid biases from an uncontrolled environment (humidity, temperature, and evaporation), the shear elasticity probe and the samples were placed in a chamber (Fig. 1). At $24°C$ the mixture was again in a liquid state and was enough viscous to avoid agar sedimentation and to keep the mixture homogeneous. Again, the ultrasonic speckle quality is dependent on the

agar particles, so if there is agar sedimentation, no ultrasonic signals are measurable. The solidification was initiated further by reducing the temperature in the chamber linearly from $24°C$ to $10°C$ in 1 hour. The chamber was made of a specifically designed electronic controller (Watlow, model 981, Winona, MN) and a refrigerator equipped with heated elements (Supra Scientifique, type YF-204017, Terrebonne, QC, Canada). Following that, the temperature was maintained at $10°C$ for 12 hours to stabilize the solidification and the mechanical properties of the gel, although gelation can go on for a longer duration [22].

B. Typical Displacement Fields

During each 13 hour experiment, a low-frequency pulse was induced, and 300 ultrasonic lines were recorded every 1 minute. The transient excitation was constituted of three consecutive low-frequency sinusoids (from 50 Hz to 200 Hz) to allow a better resolution in the frequency domain. In postacquisitions, the movement of the single-element transducer was compensated with a cross-correlation technique that used the strong echoes from the bottom of the beaker. This technique was described earlier in [16]. Then, the longitudinal component of the shear wave displacements along the ultrasonic beam was computed with a 1-D cross-correlation algorithm [23]–[25] that used successive ultrasonic signals stored in memory. Each radiofrequency scan was segmented versus depth z into 0.5 mm windows with 50% overlap. Each window corresponded to a slice within the medium. Then, during the propagation of a low-frequency impulse (from 50 Hz to 200 Hz), axial displacement of those gel slices were calculated. This technique can measure displacements of about 1 μm along the ultrasonic beam for a medium slice of approximately 1 mm [26].

In Fig. 2, displacement fields are shown at different acquisition times during the sol-gel transition process of an agar-gelatin mixture (3% agar and 2.5% gelatin). At the initial time ($t = 0$ minutes), only the bulk wave (longitudinal wave P) with a speed of about 1500 m/s was visible at each depth. Between $t = 30$ minutes and $t = 60$ minutes, the medium became solid, allowing the shear waves to propagate (quasi transversal wave S). These waves were very slow and took a certain time to arrive at each depth. The shear wave slope was relative to their velocity and, in the approximation of purely elastic solid, the velocity is directly proportional to the elasticity. During the solidification process, the shear waves accelerated, their slope increased and their amplitude remained constant for a given excitation voltage. At $t = 150$ minutes, the mixture began to be mechanically stable. The slope of the shear waves did not evolve, and some secondary waves (R) appeared. These last were surface waves converted in volumetric waves coming from the beaker sides [27]. After $t = 210$ minutes, the displacement fields were very similar and no big changes could be noticed.
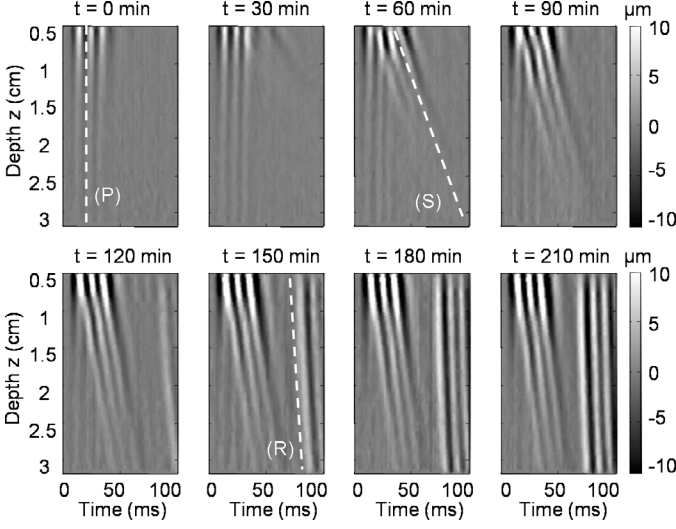
Fig. 2. Displacement field in an agar-gelatin mixture (3% agar and 2.5% gelatin) at different times (from 0 to 210 minutes) during the solidification process. The displacement field was plotted in gray color scale, along the depth z as a function of time. The low frequency pulse at 100 Hz was given at the time of 5 ms. Three different types of waves were noted: the bulk waves (P), the shear waves (S), and artifactual secondary waves (R).

C. Inverse Problem Approach

From the displacement fields, a simple inverse problem approach based on the 1-D Helmholtz equation was used to recover the shear velocity (V_S) and attenuation (α_S) of each medium [21]. This inversion is valid only in viscoelastic, homogeneous, and isotropic media. From:

$$\frac{\partial^2 FT(u_Z(z))}{\partial z^2} + k^2 FT(u_Z(z)) = 0, \qquad (1)$$

where FT is the Fourier transform, $u_z(z)$ is the longitudinal component of the shear wave displacement field, z is the depth, and k is the wave vector, then the local complex wave vector was given by:

$$k = \sqrt{\frac{\frac{\partial^2 FT(u_Z(z))}{\partial z^2}}{FT(u_Z(z))}}, \qquad (2)$$

and the local shear wave velocity V_S and shear wave attenuation α_S were expressed as [28]:

$$V_S = \frac{\omega}{\text{Re}[k]}, \quad \alpha_S = \text{Im}[k], \qquad (3)$$

with $\omega = 2\pi f$ being the pulsation frequency that varied between 50 Hz and 200 Hz.

To retrieve the medium elasticity and viscosity, we assume that the material mechanical behavior corresponds to a simple mechanical model. Here we are dealing with a material that is changing from a liquid to a solid state. The two possible simplest models are the Maxwell's (usually used for fluids) and Voigt's (usually used for solids) models [29]. As shear waves can only propagate in solids, the Voigt's model is used here [21].

A Voigt's model is composed of a spring representing the elasticity (μ) in parallel with a dashpot corresponding to the viscosity (η) [30]. From this model, the stress-strain relationship was deduced:

$$\sigma = \mu\varepsilon + \eta\frac{\partial\varepsilon}{\partial t}, \qquad (4)$$

where σ is the stress and ε is the strain. Then, because $\varepsilon = (\partial u_z/\partial z)$ and $div\sigma = \rho.g$ (g is the acceleration), one can deduce from (4), the new Helmholtz equation given by:

$$\frac{\partial^2 FT(u_z(z))}{\partial z^2} + \frac{\rho\omega^2}{(\mu + i\omega\eta)}FT(u_z(z)) = 0, \qquad (5)$$

where ρ is the density of the medium.

Thus, from the complex wave vector, the shear wave velocity as well as the shear wave attenuation can be expressed as a function of the elasticity and viscosity:

$$V_S = \sqrt{\frac{2\left(\mu^2 + \omega^2\eta^2\right)}{\rho\left(\mu + \sqrt{\mu^2 + \omega^2\eta^2}\right)}}, \qquad (6)$$

$$\alpha_S = \sqrt{\frac{\rho\omega^2\left(\sqrt{\mu^2 + \omega^2\eta^2} - \mu\right)}{2\left(\mu^2 + \omega^2\eta^2\right)}}. \qquad (7)$$

By analytically inversing (6) and (7), the elasticity μ and the viscosity η were retrieved as a function of time:

$$\mu = \frac{\rho V_S^2}{\left(\left|1 - \left(\frac{\alpha_S V_S}{\omega}\right)^2\right|\right)\left(\frac{2}{1 - \left(\frac{\alpha_S V_S}{\omega}\right)^2} - 1\right)}, \qquad (8)$$

$$\eta = \frac{\rho V_S^2}{\omega}\sqrt{\frac{\left(\frac{1}{1 - \left(\frac{\alpha_S V_S}{\omega}\right)^2} - 1\right)}{\left(\left|1 - \left(\frac{\alpha_S V_S}{\omega}\right)^2\right|\right)\left(\frac{2}{1 - \left(\frac{\alpha_S V_S}{\omega}\right)^2} - 1\right)^2}}. \qquad (9)$$

III. RESULTS AND DISCUSSION

Based on this theoretical approach, the sol-gel transition was studied as a function of the shear wave frequency, the shear wave amplitude, and the gelatin concentration.

A. Shear Wave Frequency

For four different samples (3% gelatin and 3% agar), the sol-gel transition was studied as a function of the shear wave frequency from 50 Hz to 200 Hz (Fig. 3). Because shear waves do not propagate in liquids, the assessment became valid at a precise time: t_g, when the medium was enough solid to allow the propagation of shear waves. This time was defined as the sol-gel transition time. When the samples were mechanically stable, a plateau was reached. Mean velocities and attenuations were calculated on the

TABLE I

SHEAR WAVE VELOCITIES AND ATTENUATIONS AT THE TRANSITION TIME t_g AND AT THE PLATEAU AS A FUNCTION OF THE SHEAR WAVE FREQUENCY.

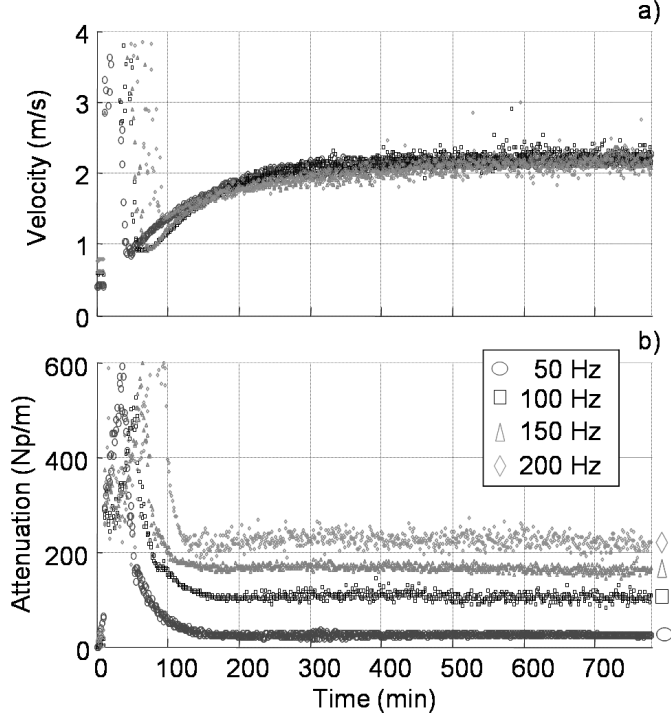| Shear wave frequency (Hz)	Time t_g (min)	Velocity at t_g: V_S (m/s)	Attenuation at t_g: α_S (Np/m)	Velocity at the plateau: V_S (m/s)	Attenuation at the plateau: α_S (Np/m)
50	42	0.88	475	2.18 ± 0.04	23 ± 1
100	57	0.92	484	2.25 ± 0.07	104 ± 8
150	70	0.96	467	2.19 ± 0.09	161 ± 7
200	98	1.37	506	2.15 ± 0.13	218 ± 13

Fig. 3. Shear wave velocity (a) and shear wave attenuation (b) as a function of time for different frequencies (from 50 Hz to 200 Hz). The gelatin mixtures for these four experiments were composed of 3% agar and 3% gelatin. The shear wave amplitude was adjusted by the minishaker voltage that was set to 4 V.

plateau over the last hour. The shear wave velocity and attenuation measurements are given in Table I.

At the precise time t_g, the shear wave velocity increased and attenuation stayed practically constant as a function of frequency (from 0.88 m/s to 1.37 m/s and from 467 Np/m to 506 Np/m, respectively). The time t_g increased from 42 minutes to 98 minutes with the shear wave frequency. This can be explained as follows: at low frequencies, the viscosity effects (directly proportional to the particle velocity, then to the frequency) are negligible when compared to the elasticity effects. In fact, it is the viscosity on elasticity ratio (also called the relaxation time) that is proportional to the attenuation by wavelength product, which determines the quality factor Q ($Q = (\eta/\mu)$) of the propagation of a wave [28]. So at a constant attenuation, larger is the wavelength, better is the quality factor, and the easier one can observe the propagation of shear waves.

At the plateau of the gelation process, the elasticity dominates. The attenuation effects were minimum, and the shear waves propagated easily. As can be seen at the beginning of the gelation process (at t_g), the medium was very soft and practically liquid. The attenuation was too important to observe shear waves (they did not propagate over more than one wavelength). One should understand that the mixtures need to reach a certain level of elasticity during the solidification to allow the shear wave's propagation. Actually one can define an attenuation threshold (the mean attenuation value at t_g, $\alpha_{SM} = 483 \pm 17$ Np/m). When this threshold is reached during the solidification, the transition point of the mixture, between liquid and solid, is near and the propagation of the shear waves occurs, which allow the assessment of the velocity and attenuation properly. In other words, when arriving close to the time t_g, the mixture is very soft and the viscosity is huge; but, because at low frequency the attenuation seen by the shear wave is smaller, the velocity and attenuation assessments can be determined sooner. So, if the shear wave frequency is sufficiently low, the attenuation is small enough to allow the propagation of the shear wave when the medium is minimally elastic.

However, as can be seen in Fig. 3, the velocity at the plateau was practically constant (close to 2.19 m/s), and the attenuation increased as a function of the frequency (from 23 ± 1 to 218 ± 13 Np/m). The velocity variations were minimum, which confirms the reproducibility of the agar-gelatin mixture preparation even if there were some possible variability in the agar-gelatin mixture concentration. Nevertheless, to compare with theoretical predictions, the Voigt's model of (4) was computed (Fig. 4, solid line). The simulation parameters were $\rho = 1100$ kg/m³, $\mu = 5234$ Pa, and $\eta = 1$ Pa.s for the density, elasticity, and viscosity, respectively. The elasticity parameter was deduced from the shear wave velocity at 50 Hz. The conformity of the theoretical and experimental velocities were in good agreement [Fig. 4(a)]. But in terms of attenuation, the experimental data (circles) were overestimated due to diffraction effects, even if the diffraction has a very low effect on the shear wave velocity in this range of frequency (50 Hz to 200 Hz) [27].

To correct the data from diffraction, a Green's function simulation in semi-infinite lossless media was used [31]. The simulation parameters were $\rho = 1100$ kg/m³,
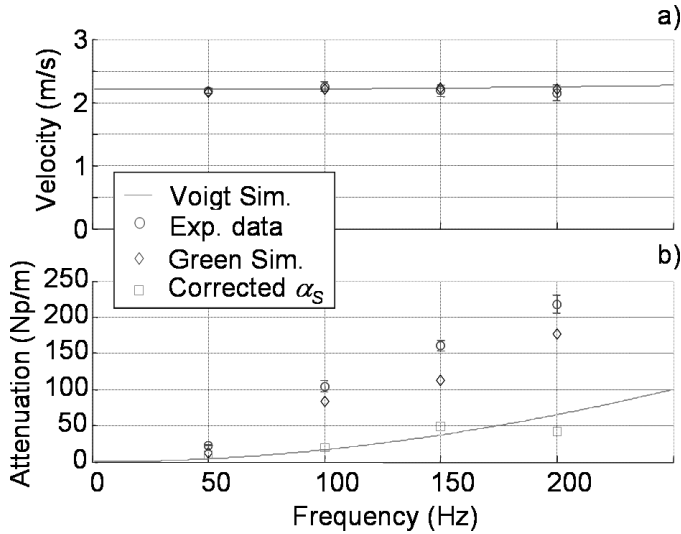
Fig. 4. Theoretical and experimental shear wave velocities (a) and shear attenuations (b) as a function of frequency. The experimental data for attenuation (○) was corrected with a Green's function simulation (◇) to compensate for the diffraction effects. The corrected attenuation α_S values (□) were in good agreement with the theoretical predictions (solid line).
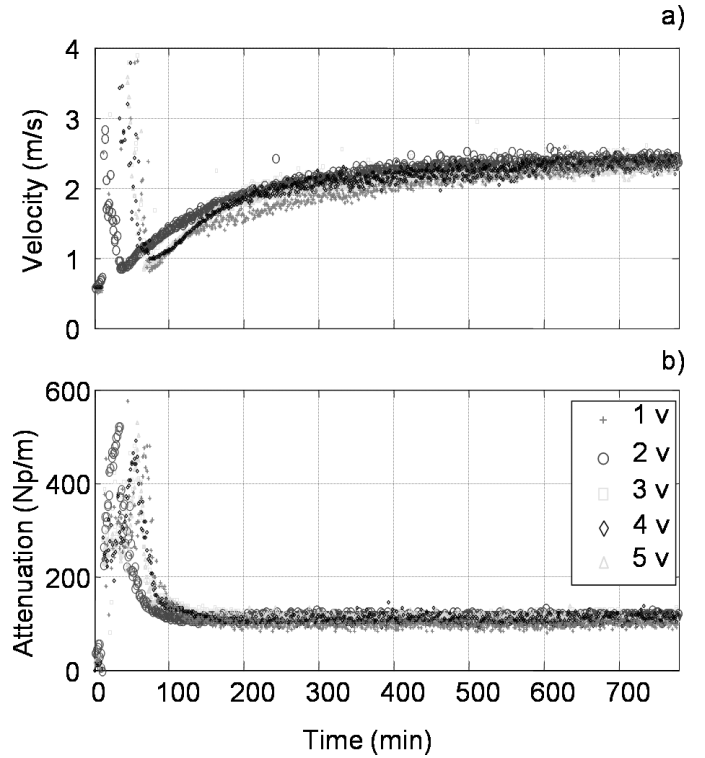

Fig. 5. Shear wave velocity (a) and shear wave attenuation (b) as a function of time for different amplitudes adjusted by the voltage on the minishaker (from 1 V to 5 V). The gelatin mixtures were composed of 3% agar and 3% gelatin. The shear wave frequency was set to 100 Hz.

$V_S = 2.19$ m/s, $V_P = 1540$ m/s, and $R = 5 \times 10^{-3}$ m for the density, shear wave velocity (mean value of the experimental data), bulk wave velocity, and piston radius (radius of the transducer). The shear wave velocities and attenuations were computed with the inverse problem approach on the simulated displacement fields (6), (7). The velocities were in good agreement with the simulation parameters and experimental data, but apparent overestimation of attenuation were still observed at each frequency. As the simulation medium was considered as lossless, the simulated attenuations should be zero. Thus, these calculated attenuations should correspond to diffraction. So, the apparent attenuations computed with the Green's function simulation (diamonds) were subtracted from the measurements, and what remains was the attenuation of the medium (squares) [21]. Consequently, the theoretical attenuations agreed with the experimental corrected data [Fig. 4(b)].

Nevertheless, as simulation methods are not a real-time process [3 days for one data point on a Pentium 4 processor (Intel, Santa Clara, CA) 3 GHz with 2 Gbytes of memory], all the following plotted attenuation assessments of the paper are relative and not absolute. In fact, the diffraction effects are correlated to the shear wavelength. As the shear velocity was changing during the gelation process, the shear wavelength was changing too. So to have a correct evaluation of attenuation during the sol-gel transition, the diffraction effects must be calculated for each velocity acquired, which is in term of simulation time not conceivable (1 experiment = 13 h ⇒ 780 × 3 days of simulation). To solve this, an exact inverse problem would be needed to compute directly the shear wave velocity and shear wave attenuation taking into account diffraction effects. However, even if the diffraction effects were not corrected, the velocity and attenuation behaviors corresponded to what could be predicted with the theoretical Voigt's model estimation.

Even if the diffraction effects are not corrected, lower is the shear wave frequency, smaller are the attenuation effects, sooner the shear waves will be observed, smaller will be the measured gelation time t_g and the measured shear wave velocity at t_g.

B. Shear Wave Amplitude

At a second time, the solidification process was studied as a function of the shear wave amplitude adjusted by the voltage of the minishaker from 1 V to 5 V at 100 Hz. For these voltage and frequency ranges, the amplifier was linear. The amplitude of the shear wave displacements induced by such a voltage were from ∼5 μm (± 2.5 μm) to ∼25 μm (±12.5 μm). Such displacements were too small and too fast to induce any significant perturbations of the medium, and they were on the order of those found in the literature with other apparatus [32].

The experiments were done on five different samples (3% gelatin and 3% agar). As shown on Fig. 5 and summarized in Table II, the shear wave velocity and the shear wave attenuation assessments were relatively constant as a function of the shear wave amplitude.

The mean velocity and attenuation values at the plateau were calculated on five experiments and were found to be

TABLE II
SHEAR WAVE VELOCITIES AND ATTENUATIONS AT THE TRANSITION TIME t_g AND AT THE PLATEAU AS A FUNCTION OF THE SHEAR WAVE AMPLITUDE.

Shear wave amplitude (V)	Time t_g (min)	Velocity at t_g: V_S (m/s)	Attenuation at t_g: α_S (Np/m)	Velocity at the plateau: V_S (m/s)	Attenuation at the plateau: α_S (Np/m)
1	73	0.80	368	2.33 ± 0.05	98 ± 4
2	34	0.86	370	2.39 ± 0.05	117 ± 5
3	68	0.92	218	2.32 ± 0.06	117 ± 7
4	57	0.92	484	2.25 ± 0.07	104 ± 8
5	66	0.84	262	2.29 ± 0.05	109 ± 5

2.31 ± 0.05 m/s and 109 ± 8 Np/m, respectively. This allows one to appreciate the reproducibility of the method, even if the shear wave velocity and shear wave attenuation measurements at t_g showed more variabilities (the mean values at t_g were: $V_{SM} = 0.87\pm0.05$ m/s, $\alpha_{SM} = 340\pm104$ Np/m, $t_{gM} = 60 \pm 15$ minutes). These variabilities may come from the agar-gelatin mixture preparation, actually the water volume, agar and gelatin weights must be measured very precisely to obtain the right concentration. In addition, the mixture temperature control is very important to assess the gel properties. The experiment must have the same temperature at the beginning to observe the same kinetics as a function of time. The mixtures were at 24°C at the beginning ($t = 0$ minutes) to avoid the agar particle sedimentation and to keep the mixtures homogeneous. For the set of measurements at 2 V, a temperature lower than 24°C was unfortunately experienced, which could explain the small time $t_g = 34$ minutes. In fact, the gelation kinetics depend directly on the temperature history as reported in the literature [9], [33]. The temperature was well controlled in the measurement chamber, but unfortunately the room temperature could vary during the preparation of samples. Nevertheless, as expected by elastic wave theory [28], the shear wave amplitude has no effects on the shear wave velocity (6) and shear wave attenuation (7) assessments.

C. Gelatin Concentration

In Fig. 6, the shear wave velocity and shear wave attenuation patterns are seen for gelatin concentrations increasing from 1.5% to 4%. For each sample, the agar concentration was 3%. The shear wave frequency and shear wave amplitude were set to 100 Hz and 4 V, respectively. Measurements are summarized in Table III.

As listed in Table III, t_g decreased from 185 minutes to 21 minutes when the gelatin concentration increased. Moreover, the shear wave velocity at the plateau varied from 0.47 ± 0.08 to 3.94 ± 0.10 m/s, whereas the attenuation changed from 184 ± 26 to 14 ± 3 Np/m. In fact, in an agar-gelatin phantom, higher is the gelatin concentration, harder is the medium. These results are in good agreement with the literature [34]–[36]. So it is not surprising to observe an increase of the velocity as the gelatin concentration increased. The decrease in attenuation also
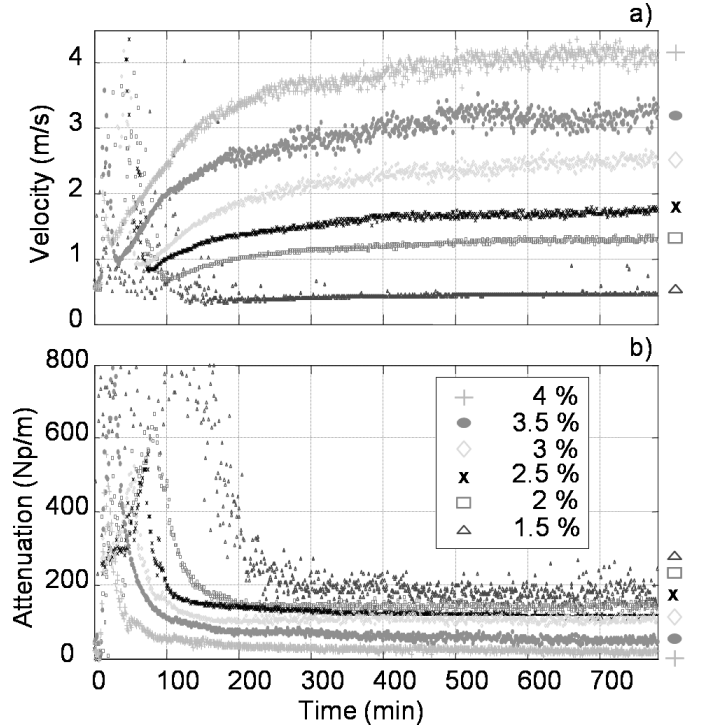

Fig. 6. Evolution of the shear wave velocity (a) and shear wave attenuation (b) at 100 Hz as a function of time for different gelatin concentrations (from 1.5% to 4%). The shear wave amplitude was constant in those measurements (the minishaker voltage was adjusted to 4 V).

is consistent. More solid is the medium (the density is constant, only the medium structure is changing); faster and less attenuated is the shear wave propagation.

At the opposite of the frequency dependence (Section III-A), the time t_g decreased as the velocity at t_g increased. The mean attenuation at t_g was about the same ($\alpha_{SM} = 456 \pm 20$ Np/m) and the frequency-attenuation ratio was almost constant ($f = 100$ Hz). The variations of velocity at t_g are due only to the gelatin concentration. So higher is the gelatin concentration, faster the medium becomes solid, and faster the elasticity of the mixture is increasing. In other words, faster is the attenuation threshold reached, defined by the mean attenuation value, faster the shear wave's propagation is observed. This confirms the dependence of the shear wave's propagation on the viscosity-elasticity ratio.

TABLE III

SHEAR WAVE VELOCITIES AND ATTENUATIONS AT THE TRANSITION TIME t_g AND AT THE PLATEAU AS A FUNCTION OF THE GELATIN CONCENTRATION.

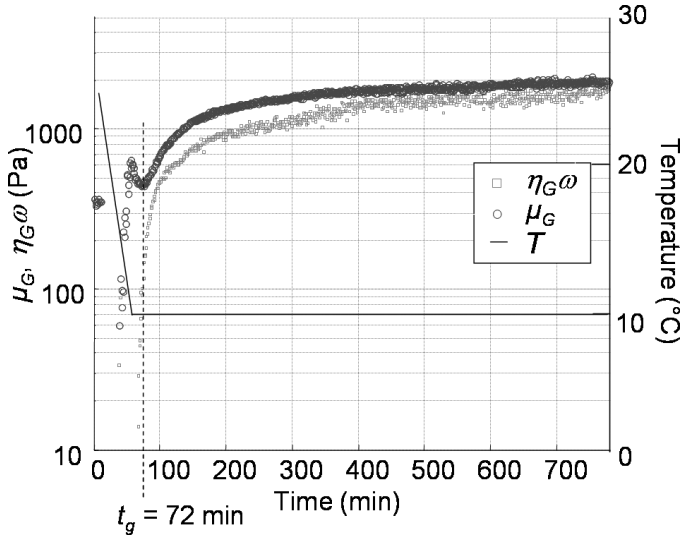| Gelatin concentration (%)	Time t_g (min)	Velocity at t_g: V_S (m/s)	Attenuation at t_g: α_S (Np/m)	Velocity at the plateau: V_S (m/s)	Attenuation at the plateau: α_S (Np/m)
4	21	1.26	454	3.94 ± 0.10	14 ± 3
3.5	36	1.01	460	3.21 ± 0.12	51 ± 6
3	57	0.92	484	2.25 ± 0.07	104 ± 8
2.5	72	0.82	423	1.72 ± 0.03	114 ± 3
2	98	0.69	466	1.29 ± 0.02	146 ± 7
1.5	185	0.32	447	0.47 ± 0.08	184 ± 26

Fig. 7. Kinetics of gelation: relative elasticity μ_G and relative viscosity η_G versus time at 100 Hz for an agar-gelatin mixture of 2.5% gelatin and 3% agar. The shear wave amplitude was adjusted by the minishaker voltage to 4 V.

At last, one can also point out the temperature influence on the sol-gel transition process. The time t_g sometimes occurred before 60 minutes, when the temperature was in transition between 24°C and 10°C in the chamber. So the shear wave velocity and shear wave attenuation assessments before 60 minutes compared to those after were not acquired under exactly the same conditions, even if the temperature decrease was always linear. So the temperature influence on the shear wave velocity and attenuation assessments for these specific measures stay an open question.

D. Elasticity, Viscosity

In Fig. 7, results are shown for a 2.5% gelatin mixture concentration. Even if the diffraction effects were not corrected, these parameters evolved as a power law, as predicted by the Winter-Chambon's criterion [5], [6]. Note that the plotted elasticity and viscosity are relative values and not absolute. The viscosities were multiplied by the pulsation frequency to match the scale. Both the elasticity and viscosity reached a maximum when the

phantom was mechanically stable [5], [6]. At the plateau, the mean values were calculated in the last hour and $\mu_G = 1.97 \pm 0.05$ kPa and $\eta_G = 2.7 \pm 0.1$ Pa.s. At t_g, $\mu_{Gtg} = 0.44$ kPa and $\eta_{Gtg} = 0.1$ Pa.s. These results are in good agreement with measurements of elasticity (defined as G') and viscosity (defined as G'') as function of time found in the literature on gelatin sol-gel transition [36]. For example, Joly-Duhamel et al. [36] found at $f = 1$ Hz, at the plateau after 5 hours and at 10°C, $G' = \mu \approx 0.7$ kPa and $G''/\omega = \eta \approx 0.8$ Pa.s [29] for a 2% gelatin concentrated mixture without agar. Study of such results with a complete inverse problem that would consider diffraction effects may eventually allow one to determine exactly the evolution of elasticity and viscosity as a function of time. These could lead one to obtain the real gelation time t_g and structural information on the gel [37]. In fact, around time t_g, the medium could be described as a polymer liquid mixture in a percolation regime. Far from t_g, the medium could be considered as an homogeneous network. The elasticity and viscosity variations also could be related to the number of polymers (helice's number) during the sol-gel transition [36].

IV. CONCLUSIONS

The transient elastography technique allows one to follow the liquid-to-solid transition (sol-gel transition) of polymer mixtures. It has been shown that the method is very sensitive to different parameters, especially to the material composition. Shear wave velocity and shear wave attenuation, related to the elasticity and viscosity of the medium, have been assessed as a function of time. The shear wave velocity increased and the shear wave attenuation decreased as a function of the gelatin concentration. These sets of experiments demonstrate the feasibility and sensitivity of the transient elastography technique to follow the transition of materials from liquid to solid state. Moreover, this technique provides a quantitative elasticity and viscosity measurement of the sol-gel transition in the audible range of frequencies compared to other techniques [11], [12].

For elasticity imaging, the so-called 1-D shear elasticity probe is relevant; but to consider viscosity diffraction

effects, the method would need to be improved by solving the exact inverse problem. Further works are needed to describe theoretically these processes through the percolation theory. Because not only chemical polymers have a sol-gel transition [38], [39], this method also can be used with biological materials, as blood for example, to better understand its solidification process during coagulation [40].

References

[1] P. E. Rouse, "A theory of the linear viscoelastic properties of dilute solutions coiling polymers," *J. Chem. Phys.*, vol. 21, no. 7, pp. 1272–1280, 1953.

[2] M. Mooney, "A diffusion theory of the visco-elasticity of rubbery polymers in finite elastic strain," *J. Poly. Sci.*, vol. 34, pp. 599–626, 1959.

[3] P. G. de Gennes, *Scalling Concepts in Polymer Physics*. Ithaca, NY: Cornell Univ. Press, 1979.

[4] B. H. Zimm, "Dynamics of polymer molecules in dilute solution: Viscoelasticity, flow birefringence and dielectrics loss," *J. Chem. Phys.*, vol. 24, no. 2, pp. 269–278, 1956.

[5] H. H. Winter and F. Chambon, "Analysis of linear viscoelasticity of a crosslinking polymer at the gel point," *J. Rheol.*, vol. 30, no. 2, pp. 367–382, 1986.

[6] H. H. Winter and F. Chambon, "Linear viscoelasticity at the gel point of a crosslinking PDMS with imbalanced stoichiometry," *J. Rheol.*, vol. 31, no. 8, pp. 683–697, 1987.

[7] A. Bleuzen, S. Barboux-Doeuff, P. Flaud, and C. Sanchez, "Rheological study of titanium oxide-based gels," *Mater. Res. Bull.*, vol. 29, no. 12, pp. 1223–1232, 1994.

[8] F. Devreux, J. P. Boilot, F. Chaput, L. Malier, and M. A. V. Axelos, "Crossover from scalar to vectorial percolation in silica gelation," *Phys. Rev. E*, vol. 47, no. 4, pp. 2689–2694, 1993.

[9] M. Djabourov, J. Leblond, and P. Papon, "Gelation of aqueous gelatin solutions: II. Rheology of the sol-gel transition," *J. Phys. France*, vol. 49, pp. 333–343, 1988.

[10] L. Klein, Ed. *Sol Gel Optics: Processing and Applications.* Boston: Kluwer Academic, 1993.

[11] G. Pucetti and R. M. Leblanc, "Direct evidence of the liquid-solid transition of a sol-gel material using photoacoustic spectroscopy," *J. Phys. Chem.*, vol. 100, pp. 1731–1737, 1996.

[12] S. Serfaty, P. Griesmar, M. Gindre, G. Gouedard, and P. Figuière, "An acoustic technique for investigating the sol-gel transition," *J. Mater. Chem.*, vol. 8, no. 10, pp. 2229–2231, 1998.

[13] D. L. Sidebottom, "Ultrasonic measurements of an epoxy resin near its sol-gel transition," *Phys. Rev. E*, vol. 48, no. 1, pp. 391–399, 1993.

[14] S. C. Ng, T. J. C. Hosea, H. C. The, and L. M. Gan, "Determination of the sol-gel transition temperature and phase diagram of a gelation system by Brillouin spectroscopy," *J. Phys. E: Sci. Instrum.*, vol. 18, pp. 250–252, 1985.

[15] I. Sack, E. Gedat, J. Bernarding, G. Buntkowsky, and J. Braun, "Magnetic resonance elastography and diffusion-weighted imaging of the sol/gel phase transition in agarose," *J. Mag. Res.*, vol. 166, pp. 252–261, 2004.

[16] L. Sandrin, M. Tanter, J.-L. Gennisson, S. Catheline, and M. Fink, "Shear elasticity probe for soft tissues with 1D transient elastography," *IEEE Trans. Ultrason., Ferroelect., Freq. Contr.*, vol. 49, no. 4, pp. 436–446, 2002.

[17] J.-L. Gennisson, S. Catheline, S. Chaffaï, and M. Fink, "Transient elastography in anisotropic medium: Application to the measurement of slow and fast shear waves velocities in muscles," *J. Acoust. Soc. Amer.*, vol. 114, no. 1, pp. 536–541, 2003.

[18] S. Catheline, J.-L. Gennisson, M. Tanter, and M. Fink, "Observation of shock transverse waves in elastic media," *Phys. Rev. Lett.*, vol. 91, no. 16, pp. 43011–43014, 2003.

[19] S. Catheline, J.-L. Gennisson, and M. Fink, "Measurement of elastic nonlinearity of soft solid with transient elastography," *J. Acoust. Soc. Amer.*, vol. 114, no. 6, pp. 3087–3091, 2003.

[20] X. Jacob, J.-L. Gennisson, S. Catheline, M. Tanter, C. Barrière, D. Royer, and M. Fink, "Study of elastic nonlinearity of soft solids with transient elastography," in *Proc. IEEE Ultrason. Symp.*, 2003, pp. 660–663.

[21] S. Catheline, J.-L. Gennisson, G. Delon, R. Sinkus, M. Fink, S. Abouelkaram, and J. Culioli, "Measurement of viscoelastic properties of soft solid using transient elastography: The inverse problem approach," *J. Acoust. Soc. Amer.*, vol. 116, no. 6, pp. 3734–3741, 2004.

[22] C. Joly-Duhamel, D. Hellio, and M. Djabourov, "All gelatin networks: 1. Biodiversity and physical chemistry," *Langmuir*, vol. 18, no. 19, pp. 7208–7217, 2002.

[23] R. J. Dickinson and C. R. Hill, "Measurement of soft tissue motion using correlation between A-scans," *Ultrasound Med. Biol.*, vol. 8, no. 3, pp. 263–271, 1982.

[24] J. Ophir, E. I. Cespedes, H. Ponneanti, Y. Yazdi, and X. Li, "Elastography: A quantitative method for imaging the elasticity of biological tissue," *Ultrason. Imag.*, vol. 13, pp. 111–134, 1991.

[25] I. A. Hein and W. D. O'Brien, "Current time domain methods for assessing tissue motion by analysis from reflected ultrasound echoes—A review," *IEEE Trans. Ultrason., Ferroelect., Freq. Contr.*, vol. 40, no. 2, pp. 84–102, 1993.

[26] W. F. Walker and G. E. Trahey, "A fundamental limit on the performance of correlation based on phase correction and flow estimation technique," *IEEE Trans. Ultrason., Ferroelect., Freq. Contr.*, vol. 41, no. 5, pp. 644–654, 1994.

[27] S. Catheline, F. Wu, and M. Fink, "A solution to diffraction biases in sonoelasticity: The acoustic impulse technique," *J. Acoust. Soc. Amer.*, vol. 105, no. 5, pp. 2941–2950, 1999.

[28] D. Royer and E. Dieulesaint, *Elastic Waves in Solid.* New York: Springer-Verlag, 1996.

[29] M. Y. Jaffin and F. Goubel, *Biomécanique Des Fluides et Des Tissues.* Paris: Masson, 1998.

[30] Y. Fung, *Biomechanics: Mechanical Properties of Living Tissue.* New York: Springer-Verlag, 1993.

[31] D. C. Gakenheimer and J. Miklowitz, "Transient excitation of an half space by a point load traveling on the surface," *J. Appl. Mech.*, vol. 36, pp. 505–514, 1969.

[32] B. Gauthier-Manuel, R. Meyer, and P. Pieranski, "The sphere rheometer: I. Quasistatic measurements," *J. Phys. E: Sci. Instrum.*, vol. 17, pp. 1177–1182, 1984.

[33] L. Payet, A. Ponton, F. Agnely, P. Colinart, and J. L. Grossiord, "Caractérisation rhéologique de la gélification d'alginate et chitosane: Effet de la température," *Rhéologie*, vol. 2, pp. 46–51, 2002.

[34] C. L. De Korte, "Intravascular ultrasound elastography," Ph.D. dissertation, Erasmus University of Rotterdam, The Netherlands, 1999.

[35] L. K. Ryan and F. S. Foster, "Tissue equivalent vessel phantoms for intravascular ultrasound," *Ultrasound Med. Biol.*, vol. 23, no. 2, pp. 261–273, 1997.

[36] C. Joly-Duhamel, D. Hellio, A. Adjari, and M. Djabourov, "All gelatin networks: 2. The master curve of elasticity," *Langmuir*, vol. 18, no. 19, pp. 7158–7166, 2002.

[37] A. Ponton, S. Warlus, and P. Griesmar, "Rheological study of the sol-gel transition in silica alkoxides," *J. Colloid Interface Sci.*, vol. 249, no. 2, pp. 209–216, 2002.

[38] E. D. Kudryashov, N. T. Hunt, E. O. Arikainen, and V. A. Buckin, "Monitoring of acidified milk gel formation by ultrasonic shear wave measurements. High-frequency viscoelastic moduli of milk and acidified milk gel," *J. Dairy Sci.*, vol. 84, pp. 375–388, 2001.

[39] F. Bakkali, A. Moudden, B. Faiz, A. Amghar, G. Maze, F. Montero de Espinosa, and M. Akhnak, "Ultrasonic measurements of milk coagulation time," *Meas. Sci. Technol.*, vol. 12, pp. 2154–2159, 2001.

[40] J.-L. Gennisson, F. Yu, and G. Cloutier, "Analysis of blood clot formation with transient elastography: Similarity with sol-gel transition in agar-gelatin phantoms," in *Proc. IEEE Ultrason. Symp.*, 2004, pp. 1134–1137.